

REPORT DOCUMENTATION PAGE			Form Approved OMB No. 0704-0188	
<small>Public reporting burden for this collection of information is estimated to average 1 hour per response, including the time for reviewing instructions, searching data sources, gathering and maintaining the data needed, and completing and reviewing the collection of information. Send comments regarding this burden estimate or any other aspect of this collection of information, including suggestions for reducing this burden to Washington Headquarters Service, Directorate for Information Operations and Reports, 1215 Jefferson Davis Highway, Suite 1204, Arlington, VA 22202-4302, and to the Office of Management and Budget, Paperwork Reduction Project (0704-0188) Washington, DC 20503.</small>				
PLEASE DO NOT RETURN YOUR FORM TO THE ABOVE ADDRESS.				
1. REPORT DATE (DD-MM-YYYY) 30-09-2014		2. REPORT TYPE Performance/Technical Report (Annual)		3. DATES COVERED (From - To) Oct. 01, 2013 - Sept. 30, 2014
4. TITLE AND SUBTITLE Enhanced Multistatic Active Sonar via Innovative Signal Processing			5a. CONTRACT NUMBER	
			5b. GRANT NUMBER N00014-12-1-0381	
			5c. PROGRAM ELEMENT NUMBER	
6. AUTHOR(S) Jian Li			5d. PROJECT NUMBER	
			5e. TASK NUMBER	
			5f. WORK UNIT NUMBER	
7. PERFORMING ORGANIZATION NAME(S) AND ADDRESS(ES) University of Florida Office of Engineering Research 343 Weil Hall, P.O.Box 116550 Gainesville, FL 32611			8. PERFORMING ORGANIZATION REPORT NUMBER	
9. SPONSORING/MONITORING AGENCY NAME(S) AND ADDRESS(ES) Office of Naval Research 875 North Randolph Street Arlington, VA 22203-1995			10. SPONSOR/MONITOR'S ACRONYM(S) ONR	
			11. SPONSORING/MONITORING AGENCY REPORT NUMBER	
12. DISTRIBUTION AVAILABILITY STATEMENT Approved for Public Release; Distribution is Unlimited.				
13. SUPPLEMENTARY NOTES				
14. ABSTRACT Pulsed active sonar (PAS) and continuous active sonar (CAS) in the presence of strong direct blast are studied for the Doppler-tolerant linear frequency modulation waveform. A comparative analysis is done between PAS and CAS based on the range-Doppler and range-compression images obtained. Further, a generalized likelihood ratio (GLR) based criterion is developed for moving target detection. CAS is further studied with a Doppler-sensitive SHAPE waveform and a weighted range-Doppler processing for CAS-SHAPE system is introduced. In-water experimentation results are provided, aimed at highlighting the merits and limitations of PAS and CAS, as well as Doppler-tolerant and Doppler-sensitive waveforms in the presence of a strong delay and Doppler-spread direct blast.				
15. SUBJECT TERMS Pulsed active sonar (PAS) , continuous active sonar (CAS), strong delay and Doppler-spread direct blast, Doppler-tolerant linear frequency modulation waveform, Doppler-sensitive SHAPE waveform, in-water experimentation results.				
16. SECURITY CLASSIFICATION OF:			17. LIMITATION OF ABSTRACT	18. NUMBER OF PAGES
a. REPORT U	b. ABSTRACT U	c. THIS PAGE U	UU	12
			19a. NAME OF RESPONSIBLE PERSON Jian Li	
			19b. TELEPHONE NUMBER (Include area code) (352) 392-2642	

Enhanced Multistatic Active Sonar via Innovative Signal Processing

Jian Li

Department of Electrical and Computer Engineering, P.O. Box 116130
University of Florida, Gainesville, FL 32611
phone: (352) 392-2642 fax: (352) 392-0044 email: li@dsp.ufl.edu

Award Number: N00014-12-1-0381

<http://www.sal.ufl.edu>

LONG-TERM GOALS

Our goal is to address fundamental signal processing research issues for enhanced multistatic active sonar systems. To effectively mitigate the reverberation problems and direct blasts encountered in shallow water, both probing waveform synthesis and adaptive receive filter design techniques should be investigated. To efficiently and accurately estimate the target positions and velocities, both target association schemes and weighted target parameter estimation methods should be devised.

OBJECTIVES

Our objectives of the current effort are to (1) develop a set of structured algorithmic approaches for both pulsed active sonar (PAS) and continuous active sonar (CAS) systems for range-Doppler and range-compression processing, and (2) to provide TREX13 in-water experimentation results aimed at highlighting the merits and limitations of PAS and CAS, as well as Doppler-tolerant and Doppler-sensitive waveforms in the presence of a strong delay and Doppler-spread direct blast.

APPROACH

Active sonar systems can have a variety of configurations namely mono-static, bi-static and multi-static. This report deals with a dataset generated from an in-water experiment where a bi-static scenario was established. Active sonar systems are further classified on the basis of the type of waveform they utilize to illuminate the region of interest. They include PAS and CAS. PAS systems work on the principle of broadcasting a low duty cycle high instantaneous power pulse into the region of interest followed by a long listening time, while the CAS systems broadcast a waveform that is characterized by a high duty cycle and low instantaneous power. PAS systems due to their high instantaneous power may have a detrimental effect on the marine life, while the CAS systems do not pose such dangers due to their low instantaneous power. CAS systems are also attractive from the point of view of having continuous access to the target, as the target is illuminated by the pulse for nearly the complete pulse repetition interval (PRI), and hence opening up the avenue for better target tracking than its PAS counterpart. In this report both the PAS and CAS systems are studied first for a particular set of probing waveforms and then the CAS system, due to its stated benefits, is investigated further.

The key individuals participating in this work include the PI, Dr. Jian Li, her Ph.D. students, Mr. Akshay Jain and Mr. Shujian Yu, and the Adjunct Research Associate Professor, Dr. Luzhou Xu, all of the University of Florida.

WORK COMPLETED

The most critical aspect of any active sonar system is the receiver and probing waveform design. The type of receiver and probing waveform to be utilized depends heavily on the type of scenario encountered by the active sonar system. In the presence of strong interference, due to multiple targets, severe clutter, and noise, the standard matched filter (MF) receiver does not provide an acceptable level of performance, and hence other receivers and waveform designs are studied for such scenarios. In this report, a simple generalized likelihood ratio (GLR) based criterion is developed which enhances the range Doppler/range compression images generated by the standard MF. Also, the Doppler-tolerant linear frequency modulation (LFM) as well as the Doppler-sensitive SHAPE waveforms are used for the investigative study being conducted here.

A set of structured algorithmic approaches are developed for both PAS and CAS systems for range-Doppler and range-compression processing and in-water experimentation results are provided, aimed at highlighting the merits and limitations of PAS and CAS, as well as Doppler-tolerant and Doppler-sensitive waveforms in the presence of a strong delay- and Doppler-spread direct blast.

RESULTS

For the TREX13 setup, the waveforms that are being investigated are the Doppler-tolerant LFM and Doppler-sensitive SHAPE waveforms. As mentioned earlier, the main tasks are to, firstly, evaluate the merits and limitations of PAS and CAS, and secondly, the merits and limitations of LFM and SHAPE waveforms. For the first task, both the PAS and CAS systems are evaluated using the LFM waveform. For the PAS system the pulse duration is only 0.5 seconds long and has a linearly time varying frequency. It must also be noted that the pulse is constant magnitude at all instants except for the time instances coinciding with the tapered regions of the pulse. For the CAS system the LFM pulse is 18 seconds long. It is important to state here that the PRI is 20 seconds long for both PAS and CAS. Hence, for the CAS system the duty cycle is 90% while its PAS counterpart has a duty cycle of 2.5%.

The range-compression images and the GLR images for the PAS-LFM system are illustrated in Figs. 1(a)-(d) and Figs. 2(a)-(c). From Figs. 1(a) and (b), it can be seen that the range-compression image for the PAS-LFM system provides a clear picture regarding the direction of motion of the target as well as the presence of clutter and noise in the environment. On observing Fig. 1(b) closely, it can be noticed that there are two returns from the target. The continuous return indicates the ping returning back after bouncing off the target, while the second return which is alternating in nature is actually transmitted by a relay placed on the target. The relay transmits back the pulse it received on every alternate ping cycle. Figs. 1(c) and (d) present the GLR images for the PAS-LFM system. The GLR images are generated by employing the GLR test (GLRT), and also they have been normalized with the maximum pixel value at 0 dB for the ease of visual understanding. Now quite clearly, one can see the target trajectory while the noise and clutter have been filtered out. Also, the GLR image in Fig. 1(c) as well as the zoomed in version of the GLR image in Fig. 1(d) show that the target changes its trajectory slightly at 500 seconds (slow-time). Next, Fig. 2(c) is a thresholded GLR image, where the threshold is set at 18 dB and has been applied on the original (not-normalized) GLR image to generate it. It can be seen that the GLRT is able to correctly detect the target even for large ranges, given that the returns

from larger ranges are significantly weaker than the ones received when the target is close to the transmitter and receiver. Fig. 2(a) illustrates the matched filter output at a single PRI (at 300 seconds, slow-time). The red arrow indicates the location of the object in that PRI. Similarly, Fig. 2(b), illustrates the GLR output at a single PRI (at 300 seconds, slow-time). Quite clearly, the GLR criterion suppresses the noise and clutter and hence, allows for improved target detection.

Next, for the CAS-LFM, Fig. 1(e) illustrates the range-compression image with Fig. 1(f) depicting the zoomed in version of it. Further, Figs. 1(g) and (h) illustrate the GLR images, which are again normalized with the maximum pixel value at 0 dB for better visual understanding, and it can be inferred that most of the interferences have been suppressed by the GLR criterion. However, looking at Fig. 2(f), which is the thresholded GLR range versus slow-time image with the threshold having been applied to the original (not-normalized) GLR image at 18 dB, one can say that for the CAS-LFM setup the GLRT does not provide as good a target detection result as for the PAS-LFM system for moving targets that are far away, and thus have weaker returns. This is because CAS-LFM is less Doppler-tolerant than PAS-LFM, and so a waveform mismatch occurs during range-compression for moving targets for CAS-LFM, which leads to weakened moving target returns and reduced moving target detection range for CAS-LFM. On the other hand, for the PAS-LFM waveform, which is highly Doppler-tolerant, range compression does little to weaken the moving target returns, which leads to a very good moving target detection range. Next from Figs. 2(d) and (e), where a single PRI output for both MF and GLRT are depicted, it can be reiterated that GLRT helps suppress the noise and interference thus helping the receiver to improve its target detection ability. Now, as discussed earlier, compared to PAS-LFM, the CAS-LFM system due to its Doppler sensitivity is susceptible to waveform mismatch, and thus producing weaker moving target returns, which leads to shortened moving target detection range. So, in order to improve its target detection performance, it becomes essential to utilize the Doppler features of the returned ping. And so to do the same, the range-Doppler processing algorithm is utilized. Figs. 3(a)-(i), illustrate the various results obtained for the CAS-LFM system after range-Doppler processing.

Figs. 3(a)-(d), illustrate the range-Doppler imaging results that are obtained for the CAS-LFM system. From Figs. 3(c) and (d), it can be clearly seen that when the matched filter is not matched to the correct velocity of the target, which in this case is -1.90m/s , the return from the target gets buried in the clutter and noise sidelobes. However, when the MF is correctly matched to the target velocity, as in Fig. 3(d), the target return is correctly identified and hence the target detection is improved as compared to its range-compression version. This is so again because the CAS-LFM waveform exhibits some degree of Doppler sensitivity. Further, Figs. 3(e)-(h) illustrate the GLR images obtained for the range-Doppler processing of CAS-LFM system, where Figs. 3(e) and (f) are normalized GLR images with their maximum pixel value at 0 dB. The GLRT again demonstrates its credentials as a robust target detection procedure, as it eliminates the surrounding noise and clutter effectively. From Figs. 3(g) and (h), the point that matching the MF correctly to the true target velocity of $v = -1.90\text{m/s}$ produces better target detection is further enforced as a 5 dB gain is observed when the range-Doppler processing is carried out. Thus, clearly the advantages of using range-Doppler processing for CAS-LFM can be seen from the results obtained. Now, since the target velocity is unknown beforehand in practice, in order to construct the GLR image, GLRT is applied to each Doppler bin of interest. Fig. 3(i) shows the GLRT results for all the Doppler bins of interest plotted on top of each other, and have been thresholded at 18 dB. Consequently from Fig. 3(i), it can be inferred that GLRT together with range-Doppler processing provides robust target detection even at very large ranges. Further when Fig. 3(i) is compared to Fig. 2(f), a clear improvement in the target detection performance is observed for the CAS-LFM system. Thus, the merits of utilizing the Doppler space for the purpose of target detection for CAS-LFM are

visible. However, as mentioned earlier it is accompanied by an increase in computational demand, since it now includes an extra dimension to search for the target. Also, from Figs. 3(h) and 2(b), it can be observed that both PAS and CAS provide similar target detection performance. Hence, with proper processing the CAS system can provide performance which is similar to the PAS system. However, from the results illustrated in Figs. 2(c) and 3(i), clearly one can see that PAS provides slightly better target detection performance than the CAS system in the presence of the strong direct blast. The main advantage that PAS possesses is the short pulse duration and hence a short non-zero autocorrelation time.

Figs. 4 (a)-(f) represent the results obtained from the in-water experimentation data with the CAS-SHAPE system, where the target is moving towards the transmitter and receiver. Figs. 4(a)-(c) represent the GLR images, normalized with their maximum pixel values at 0 dB, obtained for the weighted range-Doppler processing performed on the CAS-SHAPE system. Quite clearly, the target as well as the direct blast can be observed in the GLR images. Using Figs. 4(a)-(c), the velocity estimate for the target as well as its position can be determined. Now from the range-Doppler images obtained, in each PRI at each delay point on the range axis, the maximum return is chosen and then the range-Doppler plane is collapsed onto the range versus slow-time plane. And hence, in this way the range versus slow-time image is generated and is illustrated in Fig. 4(d). It can be seen that the processing algorithm for the CAS-SHAPE system provides a good target detection performance. Further, from Fig. 4(f), which is generated by thresholding the original (not-normalized) GLR image at 18 dB, the target range can be known without any bias, i.e., per PRI there is only one unique range estimate, leaving aside the returns from the transponder on the boat. However while observing Fig. 3(i), it can be said that there is an ambiguity in range estimation due to the thickness of the target detection line. This is due to the ridge induced range-Doppler ambiguity associated with the Doppler-tolerant LFM waveforms, as the same target is detected with GLR exceeding 18 dB in multiple range-Doppler bins, making it harder to resolve the target and the repeater. It can be concluded that the CAS-SHAPE system provides with a more accurate target range estimation capability and a much more accurate per-PRI velocity estimate than the CAS-LFM system and so, clearly the superior performance of the adaptive variance scaling range-Doppler processing strategy for the CAS-SHAPE over that of the conventional range-Doppler processing strategy for the CAS-LFM system is demonstrated.

Another important observation to be made here is that the instantaneous full bandwidth requirements for the probing waveform can be met effectively by the SHAPE waveform. In contrast, the LFM does not permit the use of 2 seconds of silence period which the CAS-SHAPE setup utilizes. This is because the effective bandwidth for the LFM is reduced by a factor of 9 when exploiting the silence interval of the probing ping. And since the range resolution is inversely proportional to the effective signal bandwidth, it thus becomes clear that reducing the effective signal bandwidth degrades the range resolution. And so, for the current study, the range resolution for the LFM waveform with the weighted range-Doppler processing strategy is reduced by a factor of 9 as compared to that with the conventional range-Doppler processing strategy. Also, the reduced amount of observation time can lead to a decrease in SNR which can lead to a reduction in target detection range of the CAS-LFM setup, thus reinforcing the fact that the CAS-LFM setup would provide degraded results with the weighted range-Doppler processing strategy devised for CAS-SHAPE.

IMPACT/APPLICATIONS

The littoral submarines are small, quiet, and non-nuclear, making active sonar an essential technology needed for their detection. Enhancing the multistatic active sonar network's capability through

innovative waveform synthesis and receive filter design is critical to improving the Navy's ability to conduct anti-submarine warfare.

Based on the TREX13 experimental setup, where the transmitter and receiver are in close proximity while the target is far away, and results obtained, it is clear that PAS-LFM setup has better target detection capability than the CAS-LFM/SHAPE setups. Also, for the CAS-LFM system the range-Doppler processing approach results in better target detection performance than the range-compression processing approach. This is because CAS-LFM is less Doppler-tolerant than PAS-LFM. Hence, utilizing the Doppler processing for CAS-LFM becomes essential to improving the detection performance of CAS systems. Further, the Doppler-sensitive SHAPE waveforms can provide attractive features to the CAS applications. We have studied the CAS-SHAPE setup and its merits and limitations. During the course of experimenting with the CAS-SHAPE system, it has become evident that the conventional range-Doppler processing does not perform well for the CAS-SHAPE setup. However, with a weighted range-Doppler processing algorithm, unbiased and accurate range and velocity estimates are obtained for the CAS-SHAPE system. Also, when compared to the CAS-LFM system, the CAS-SHAPE systems provide a better performance in terms of range and velocity estimates. Moreover, the SHAPE ping sounds like snapping shrimps making a symphony, hence making it harder to detect by the foe than its LFM counterpart.

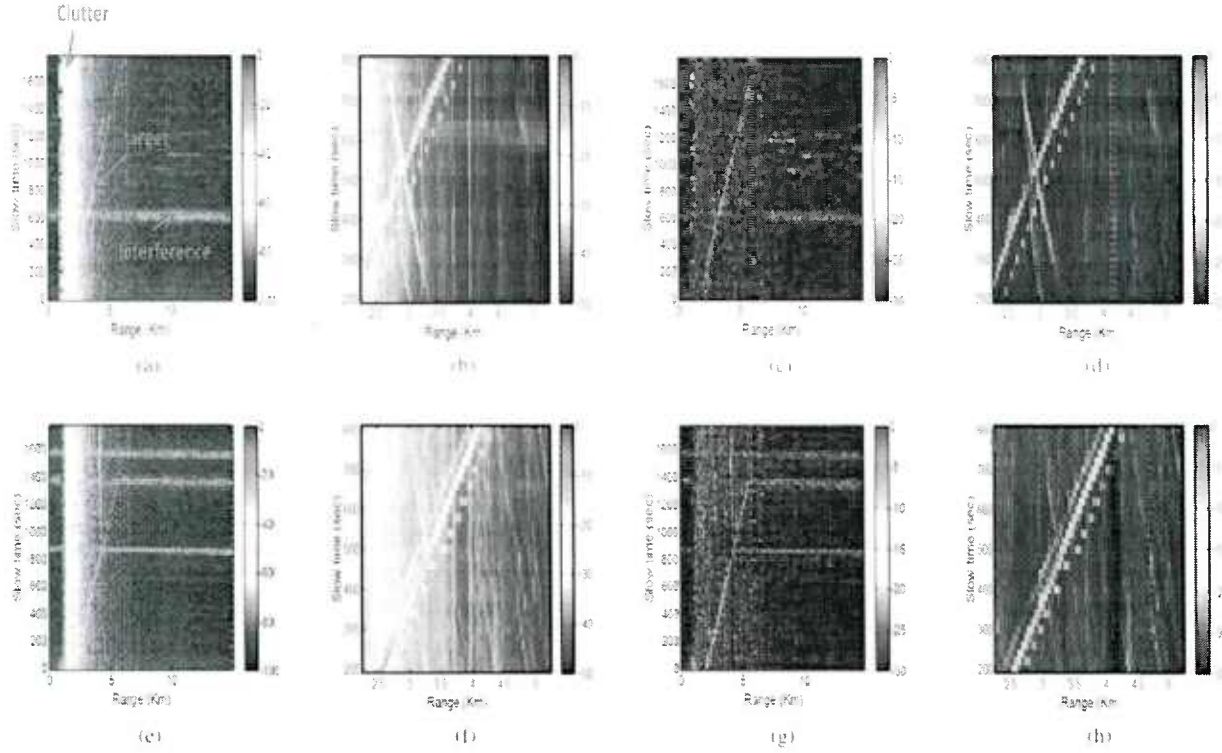


Figure 1. (a) Range compression image for PAS-LFM. (b) Zoomed in view of the range-compression image for PAS-LFM. (c) GLR image for PAS-LFM. (d) Zoomed in view of the GLR image for PAS-LFM. (e) Range-compression image for CAS-LFM. (f) Zoomed in view of the range-compression image for CAS-LFM. (g) GLR image for CAS-LFM. (h) Zoomed in view of the GLR image for CAS-LFM.

[graph: PAS-LFM offers slightly better performance than CAS-LFM with range compression only, since the CAS-LFM waveform is more Doppler sensitive than the PAS-LFM waveform.]

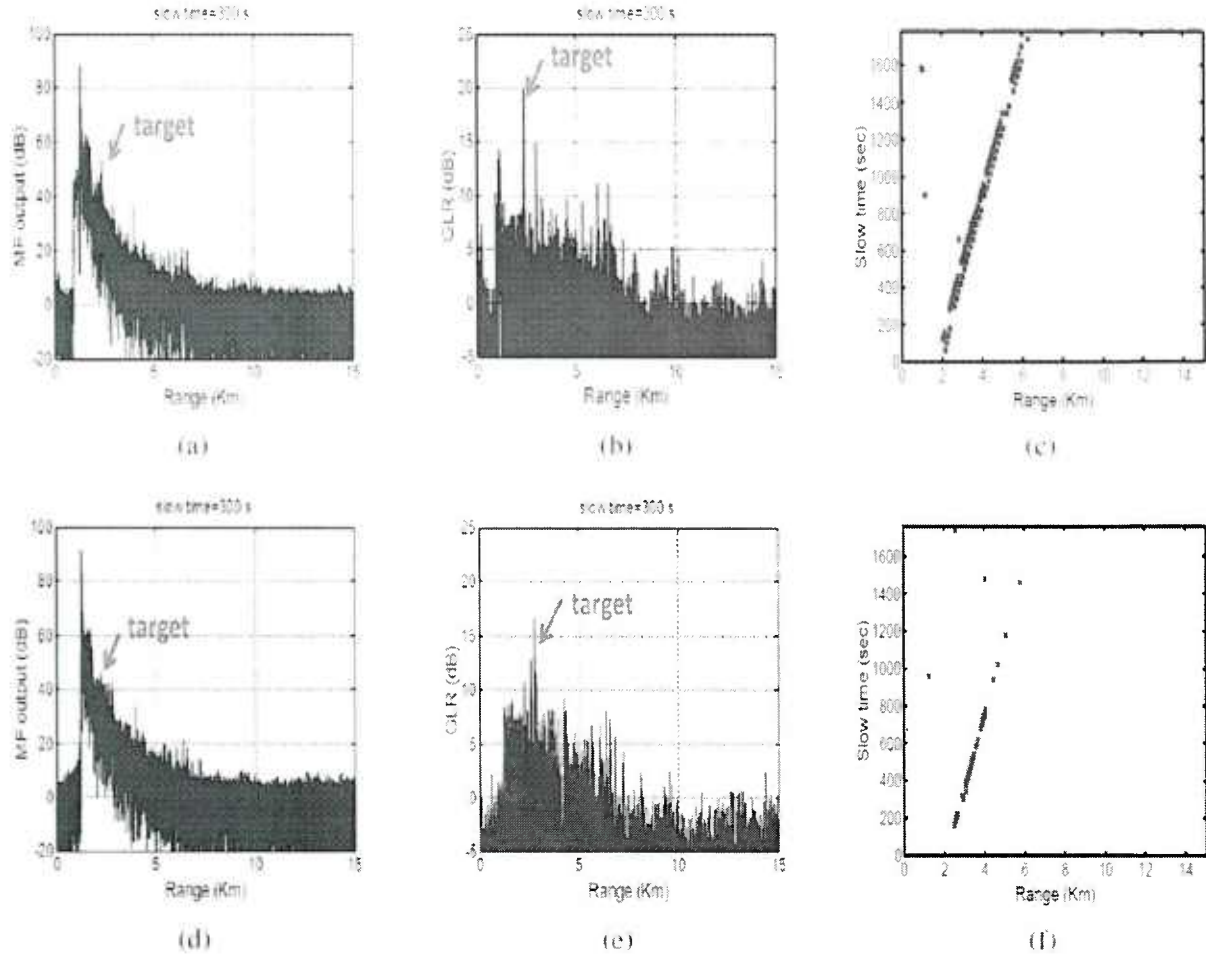


Figure 2. (a) Matched filter output power plot for a single PRI for PAS-LFM. (b) GLR output power plot for a single PRI for PAS-LFM. (c) GLR for PAS-LFM thresholded at 18dB. (d) Matched filter output power plot for a single PRI for CAS-LFM. (e) GLR output power plot for a single PRI for PAS-LFM. (f) GLR for CAS-LFM thresholded at 18dB.

[graph: Generalized likelihood ratio testing significantly enhances target detection performance.]

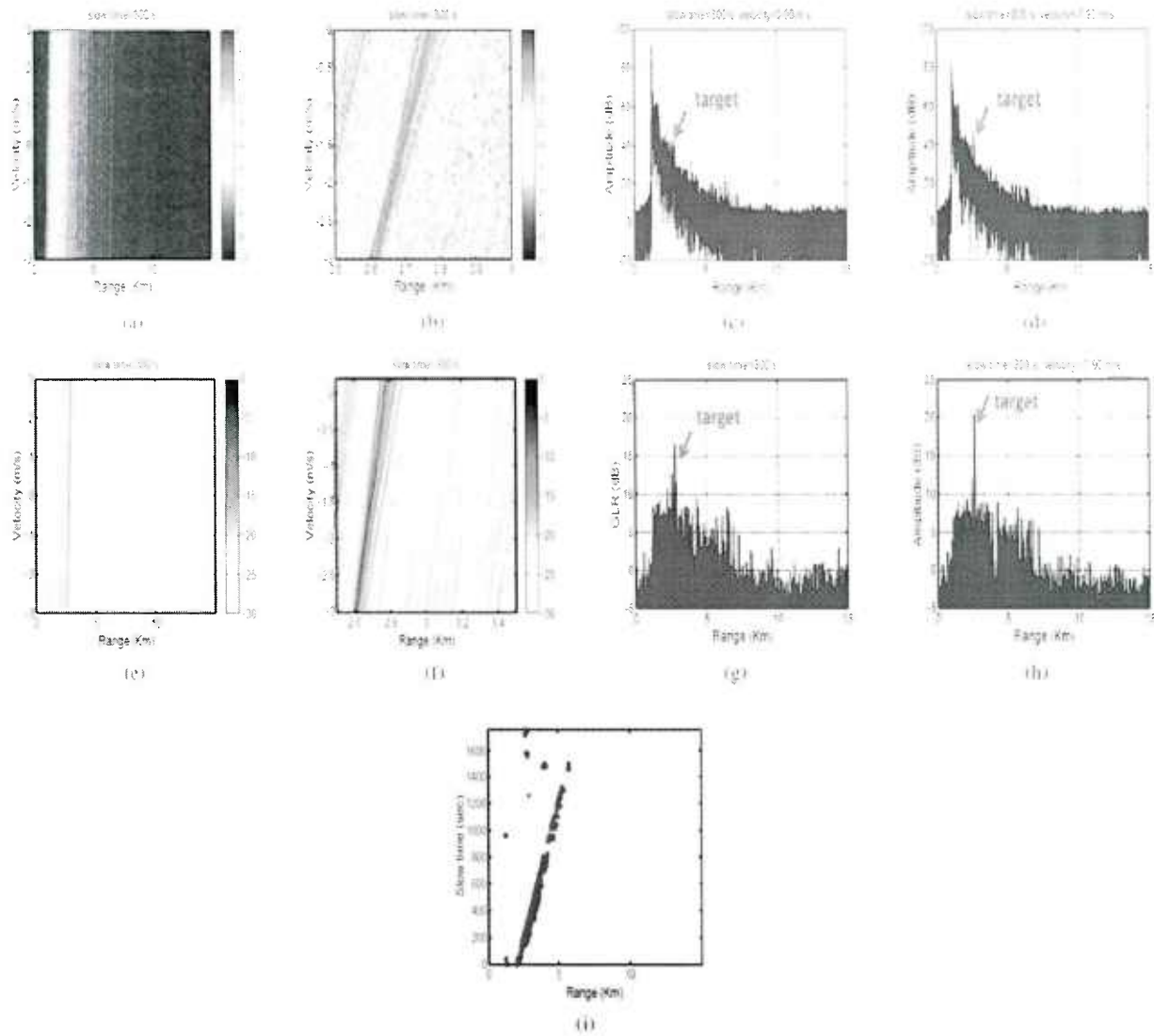


Figure 3. (a) Range-Doppler image for the CAS-LFM system. (b) Zoomed in view of the range-Doppler image for CAS-LFM system. (c) Matched filter output power at a single PRI with zero target velocity. (d) Matched filter output power at a single PRI with $v=-1.9$ m/s. (e) GLR image for range-Doppler processing for CAS-LFM. (f) Zoomed in view of the GLR image for CAS-LFM. (g) GLR output power at a single PRI with zero target velocity. (h) GLR output power at a single PRI with $v=-1.9$ m/s. (i) GLR based target detection with range-Doppler Processing for CAS-LFM systems thresholded at 18dB.

[graph:Range-Doppler processing can enhance the moving target detection for CAS-LFM due to the Doppler sensitivity of the CAS-LFM waveform.]

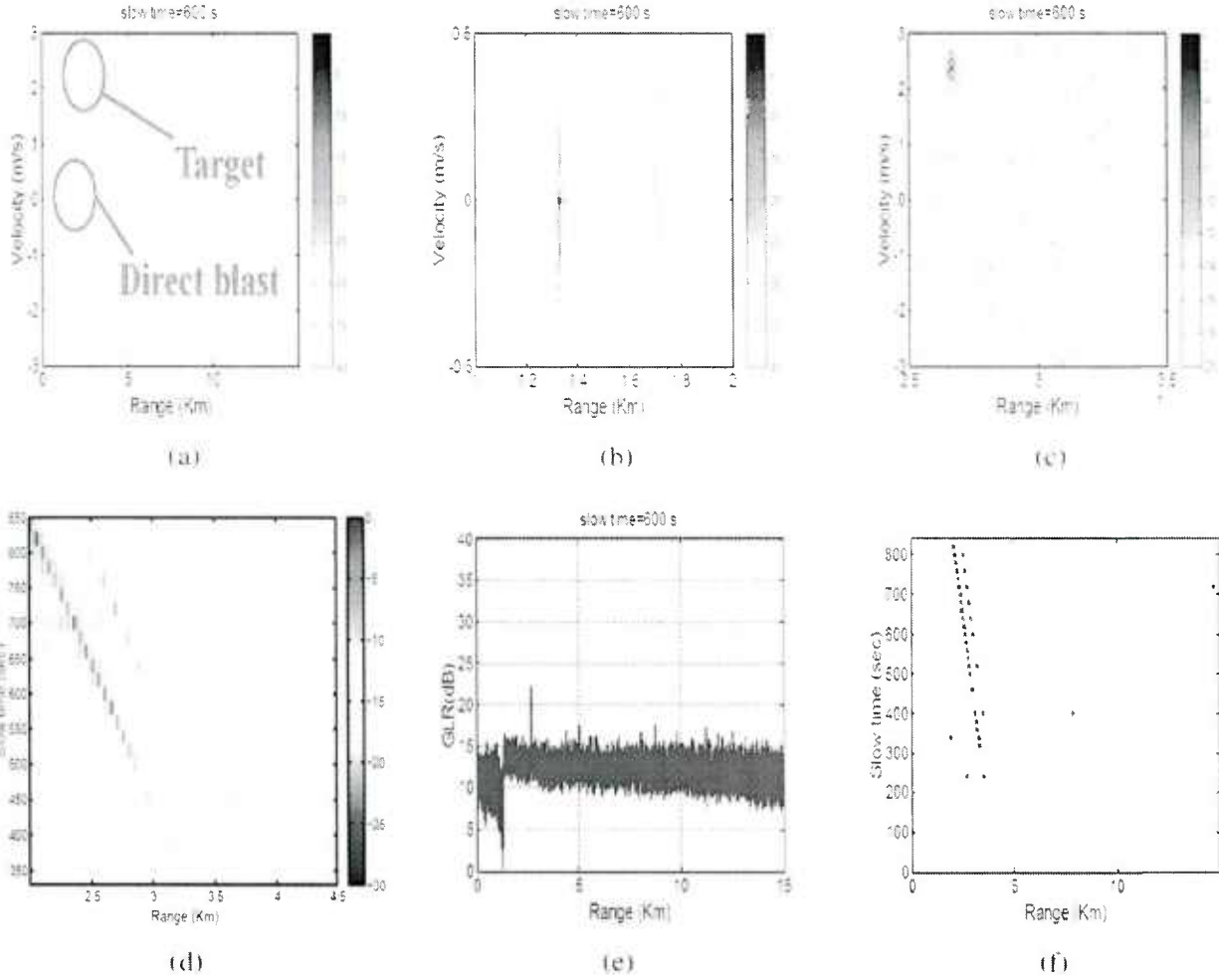


Figure 4. (a) Range-Doppler GLR image for the CAS-SHAPE system with the target and direct blast. (b) Zoomed in view of the range-Doppler GLR image for CAS-SHAPE system illustrating the direct blast. (c) Zoomed in view of the range-Doppler GLR image for CAS-SHAPE system illustrating the target return. (d) Range versus slow-time image for CAS-SHAPE. (e) Matched filter output power for single PRI for CAS-SHAPE matched at true target velocity $v = 2.5\text{m/s}$. (f) Range versus slow-time GLR image thresholded at 18 dB.

[graph:Range-Doppler processing is required for the Doppler-sensitive CAS-SHAPE waveform. Generalized likelihood ratio testing significantly enhances target detection performance. The Doppler-sensitive CAS-SHAPE waveform eliminates range-Doppler ambiguity.]

TRANSITIONS

We have provided several CAN sequences to Dr. Michael S. Datum of the Applied Physical Sciences Corporation. He has used some of the sequences as active sonar probing sequences and generated simulated datasets for ASW scenarios using the sonar simulation toolset (SST). He has also used the sequences for in-water experimentations.

We have participated the TREX-CAS in-water experimentation in 2013. We have gained much experience and insights analyzing the experimental data collected during the experimentation.

We have sent our probing waveform synthesis papers to Dr. James Alsup (alsup@cox.net) and our IAA papers to Dr. Roy Streit (streit@metsci.com).

We have also sent our presentation slides for the 2013 IEEE Underwater Acoustic Signal Processing Workshop to Dr. Don Russo (donato.russo@navy.mil) of Naval Air Warfare Center and Dr. Michael Janik (Michael_F_Janik@raytheon.com) of Raytheon Integrated Defense Systems.

RELATED PROJECTS

NONE.

PUBLICATIONS

Book

H. He, J. Li, and P. Stoica, *Waveform Design for Active Sensing Systems -- A computational approach*, Cambridge University Press, 2012. [published, refereed].

Journal Publications

K. Zhao, J. Liang, J. Karlsson, and J. Li, "Enhanced Multistatic Active Sonar Signal Processing," *The Journal of the Acoustical Society of America*, Vol. 134, No. 1, pp. 300-311, July 2013. [published, refereed].

L. Xu, K. Zhao, J. Li, and P. Stoica, "Wideband Source Localization Using Sparse Learning via Iterative Minimization," *Signal Processing*, Vol. 93, No. 12, pp. 3504-3514, December 2013. [published, refereed].

J. Ling, L. Xu, and J. Li, "Adaptive Range-Doppler Imaging and Target Parameter Estimation in Multistatic Active Sonar Systems," *IEEE Journal of Oceanic Engineering*, Vol. 39, No. 2, pp.

290-302, April 2014. [published, refereed].

W. Rowe, P. Stoica, and J. Li, "Spectrally Constrained Waveform Design," *IEEE Signal Processing Magazine*, Vol. 31, No. 3, pp. 157-162, May 2014. [published, refereed].

J. Liang, L. Xu, J. Li, and P. Stoica, "On Designing the Transmission and Reception of Multistatic Continuous Active Sonar Systems," *IEEE Transactions on Aerospace and Electronic Systems*, Vol. 50, No. 1, pp. 285-299, May 2014. [published, refereed].

L. Xu, J. Li, and A. Jain, "Impact of Strong Direct Blast on Active Sonar Systems," *IEEE Transactions on Aerospace and Electronic Systems*, to appear. [in press, refereed].

Conference Publications

K. Zhao, J. Liang, J. Karlsson, and J. Li, "Enhanced Multistatic Active Sonar Signal Processing," *IEEE International Conference on Acoustics, Speech and Signal Processing (ICASSP)*, Vancouver, Canada, May 26-31, 2013. [published, refereed].

J. Li, "On Designing the Transmission and Reception of Multistatic Continuous Active Sonar Systems," *2013 IEEE Underwater Acoustic Signal Processing Workshop*, West Greenwich, Rhode Island, October 16-18, 2013. [invited]

W. Rowe, J. Li, and P. Stoica, "Spectrally Constrained Waveform Design for MIMO Systems," *IEEE International Microwave Symposium*, Tampa Bay, FL, June 2014. [invited]

L. Xu, J. Li, and A. Jain, "Active Sonar Transmission Strategies in the Presence of Strong Direct Blast", 48th Asilomar Conference on Signals, Systems and Computers, Pacific Grove, CA, November, 2014. [in press, refereed].

HONORS/AWARDS/PRIZES

Dr. Jian Li gave a plenary talk at the IEEE Sensor Array and Multichannel Signal Processing Workshop, in Hoboken NJ, in June 2012.

Dr. Jian Li is a co-author of the following paper that received the 2013 IEEE Signal Processing Society Best Paper Award:

Amir Beck, Petre Stoica and Jian Li, "Exact and Approximate Solutions of Source Localization Problems," *IEEE Transactions on Signal Processing*, Volume: 56, No. 5, May 2008.
<http://ieeexplore.ieee.org/stamp/stamp.jsp?tp=&arnumber=4472183>